PCCP

PAPER

View Article Online
View Journal | View Issue

Cite this: *Phys. Chem. Chem. Phys.*, 2015, **17**, 261

Electrochemical studies of decamethylferrocene in supercritical carbon dioxide mixtures

Jack A. Branch, David A. Cook and Philip N. Bartlett*

Received 8th October 2014,
Accepted 7th November 2014

DOI: 10.1039/c4cp04545a

www.rsc.org/pccp

Detailed analysis of the voltammetry of decamethylferrocene at micro and macrodisc electrodes has been carried out in $scCO_2$/MeCN (15 wt%), 20 mM $[NBu^n_4][BF_4]$ and 309 K and 17.5 MPa. A passivating film needs to be removed from platinum electrodes before stable, reproducible voltammetry can be obtained. At low concentrations (0.22 mM) reversible $1e^-$ behaviour is observed. Significant effects from natural convection are also present and it is demonstrated that fitting a baffle to the electrode dampens this effect. Limiting currents at microdisc electrodes at concentrations ranging from 0.22 to 11 mM and radii of 10 to 25 μm all obey the microdisc equation. The diffusion coefficient is calculated to be 4.06×10^{-5} cm^2 s^{-1} in $scCO_2$/MeCN (15 wt%) with 20 mM $[NBu^n_4][BF_4]$ and 309 K at 17.5 MPa. The solubility of decamethylferrocene is in excess of 11 mM for these conditions.

1. Introduction

Although there have been relatively few studies of electrochemistry in supercritical solvents[1] recent studies show that these electrolytes may be of interest for applications ranging from voltammetric analysis,[2–10] electrochemical reduction of CO_2 to a variety of products,[7,11,12] electrosynthesis[13–15] and electrodeposition.[16] Interest in the applications to electrodeposition arises because of the advantages of high mass transport and the absence of surface tension which allow for the electrodeposition into high-aspect ratio nanopores and nanostructures. Thus we have studied the electrodeposition of Cu,[17] Ag[18] and Ge[19] from supercritical fluids. Given these potential practical applications it is of interest to better understand the physical chemistry and basic electrochemical processes in supercritical fluid electrolytes.

Carbon dioxide is a widely used supercritical fluid (SCF)[4,19–33] because it is non-toxic, inexpensive and non-flammable and because like all SCF its solvent properties can be tuned by variation of T and p. Supercritical carbon dioxide ($scCO_2$), although having a low dielectric constant ($\varepsilon < 2$),[4] is of interest as a supercritical solvent for electrochemistry because it is reasonably inert and because it has an easily accessible critical temperature and pressure (T_c = 304 K, p_c = 7.3 MPa). One way to increase the dielectric constant and to make it more suitable for electrochemistry is to add a more polar co-solvent.

Previously we described the phase behaviour and conductivity of multi component mixtures using $scCO_2$ (ref. 30) with both methanol and acetonitrile (MeCN) as co-solvents. Of the two, acetonitrile was found to be preferred since, for similar pressures and temperatures, the solubility of the tetraalkylammonium tetrafluoroborate supporting electrolyte was 5 times higher in acetonitrile mixtures compared to methanol.[30]

In a recent paper, Toghill *et al.*[7] reported the results of a study of voltammetry at macroelectrodes in supercritical CO_2 containing acetonitrile. In their experiments they used decamethylferrocene as the redox probe in a supercritical mixture of carbon dioxide with up to 0.41 mole fraction acetonitrile and tetradecylammonium tetrakis(pentafluorophenyl)borate (TDATFPB, a room temperature ionic liquid) as the supporting electrolyte. Based on the observed voltammetry of the decamethylferrocene at gold macrodisc electrodes they concluded that the electrochemistry occurred in a separate 60 μm thick liquid-like film of acetonitrile, CO_2 and the electrolyte present on the surface of the Au electrode. We were therefore prompted to see if this was a more general phenomenon and to look closely at the voltammetry in $scCO_2$/MeCN under our conditions (0.15 wt%, 0.17 mole fraction (CO_2/MeCN) 0.006 mole fraction (MeCN/TBATFB) acetonitrile with tetraalkylammonium tetrafluoroborate electrolyte) to see if there is evidence for the presence of such a film at the electrode surface.

In this paper we present our results using decamethylferrocene as an outer sphere redox probe to investigate the electrochemistry at both micro and macroelectrodes. We determine the diffusion coefficient through microelectrode analysis and we present evidence that indicates that in our system there is no evidence for a liquid like film present at the surface of the Pt micro disc or at an Au macro disc electrode.

School of Chemistry, University of Southampton, Southampton, UK SO171BJ. E-mail: P.N.Bartlett@soton.ac.uk

2. Experimental

2.1 Reagents

Tetrabutylammonium tetrafluoroborate ($[NBu^n_4][BF_4]$) was purchased from Aldrich and was used without further purification. Decamethylferrocene ($C_{20}H_{30}Fe$) was purchased from Aldrich and sublimed before use. Acetonitrile (MeCN) was purchased from Rathburn Chemicals and was refluxed over CaH_2 before use. CO_2 (99.9995%) was purchased from BOC. Hexaammineruthenium(III) chloride ($Ru(NH_3)_6Cl_3$) was purchased from Aldrich and used without further purification.

2.2 Electrochemical experiments

Cyclic voltammetry was performed using a potentiostat, Autolab, PGSTAT101 (Eco Chemie).

Working electrodes were platinum microdiscs (20, 25 and 50 μm diameter) sealed in glass, then further sealed in 1/16″ O.D PEEK tubing. The radii of the working microelectrodes were confirmed using scanning electron microscopy (SEM).

The ''baffle'' working electrode was a platinum microdisc (50 μm diameter) sealed in glass, then further sealed in 1/16″ O.D PEEK tubing. In addition, 1/16″ O.D PEEK tubing was placed over the working end of the electrode and extended for a further 5 mm to create a baffle around the electrode. Counter electrodes were 0.5 mm diameter Pt wires (sealed in 1/16″ O.D PEEK tubing). Reference electrodes were 0.5 mm diameter Pt wires (sealed in 1/16″ O.D PEEK tubing). The cell employed for the electrochemistry was a two-piece stainless steel construction. The bottom part has a 8.65 cm^3 well, that forms the working volume of the cell. The top part has 7, 1/16″, female, SSI type fittings, through which the electrodes, thermocouple and tubing could be sealed into the cell, along with an additional port for a safety key. The two pieces are sealed using a disposable O-ring, which are then further sealed with a safety belt, which is locked by the safety key, see our recent perspective article for more details.[16]

Electrolytes and metallocenes were introduced into the cell either as dry powders or solutions in acetonitrile. This loading step was carried out in a dry, dinitrogen-purged glove box when air sensitive materials were employed. To introduce DMFc into the supercritical cell, small quantities of the solid were weighed out and then transferred to the N_2 purged glove box. Once in the N_2 purged glove box, the DMFc was dissolved in acetonitrile. The acetonitrile itself was weighed out in the glove box to obtain the correct wt% (small errors can be introduced by this procedure as small changes in pressure in the glove box can affect the weight reading). For higher concentrations of DMFc (where tens of milligrams are required), the solid DMFc was introduced into the supercritical cell directly. For $scCO_2$–MeCN mixtures, the cell was preheated to the desired temperature by immersing in a water bath. The water bath was heated thermostatically using a heated water circulator (TC120, Grant). Supercritical fluid grade CO_2 (99.9995%, BOC) was then added *via* a specialised CO_2 pump (PU-1580-CO_2, JASCO). CO_2 was pumped at rates from 0.1–2.0 $cm^3\ min^{-1}$ (to ensure the cell temperature remained constant) until the desired pressure and CO_2 : MeCN ratio was achieved. The system was also stirred during pumping, using a magnetic stirrer, to ensure that the solution was homogenous. Stirring was stopped at least 5 min before any electrochemical measurements to allow the solution to settle.

3. Results and discussion

We have recently studied the phase behaviour and conductivity of $scCO_2$ with acetonitrile as a co-solvent and tetrabutylammonium tetrafluoroborate as supporting electrolyte.[30] In that paper we located the phase boundary for the single phase region. For the compositions similar to those used here that boundary lies at around 7.5 MPa at 309 K and increases linearly with temperature with a slope of around 0.375 MPa K^{-1}. Consequently for all the experiments described below we will be well into the single phase region around 10 MPa above the boundary.

3.1 Electrode preconditioning

Decamethylferrocene (DMFc) was chosen as the redox probe in these experiments as it was found to be better behaved than ferrocene itself and has greater stability against reactions with any trace oxygen present.[34] Preliminary results recorded at a 25 μm diameter Pt microdisc showed an electrochemical process at 0 V, but instead of reaching a limiting current on scanning anodically the current continued to increase, Fig. 1A. This behaviour was seen for all three sizes of Pt microdisc (20, 25 and 50 μm diameter). The voltammetry in Fig. 1A is suggestive of the presence of a semi porous blocking film at the electrode surface. Upon cycling the electrode within the solvent potential window (−0.2 V to 3 V then to −3 V, Fig. 1B) the voltammetry changes and the expected microelectrode redox wave is seen with a well-defined plateau. We attribute this change to the formation of a film on the electrode that is removed upon cycling over a wider potential range.

To investigate over which region the film was removed from the surface the potential range of the conditioning cycle was altered. When the electrode was cycled from −0.2 V to 3 V the film was not removed and the voltammetry was unchanged. However when the conditioning cycle was set between −0.2 V to −3 V the film was removed and well behaved DMFc voltammetry was obtained as shown Fig. 1A curve 2. We can therefore conclude that the blocking film at the electrode was removed by reduction.

Once this preconditioning step was performed on an electrode, reproducible and stable voltammetry was seen and the preconditioning step did not need to be repeated during that experimental session. A similar problem was encountered by Crooks and Bard[2] when using ferrocene in supercritical acetonitrile. There they reported the presence of a passivating layer at the tungsten working electrode that could be removed by a short voltage pulse, but which did not affect subsequent electrochemical measurements. This layer was attributed to the formation of a polymer of acetonitrile on the electrode surface. It is important to note that in these experiments it is not possible to polish the electrodes immediately before recording

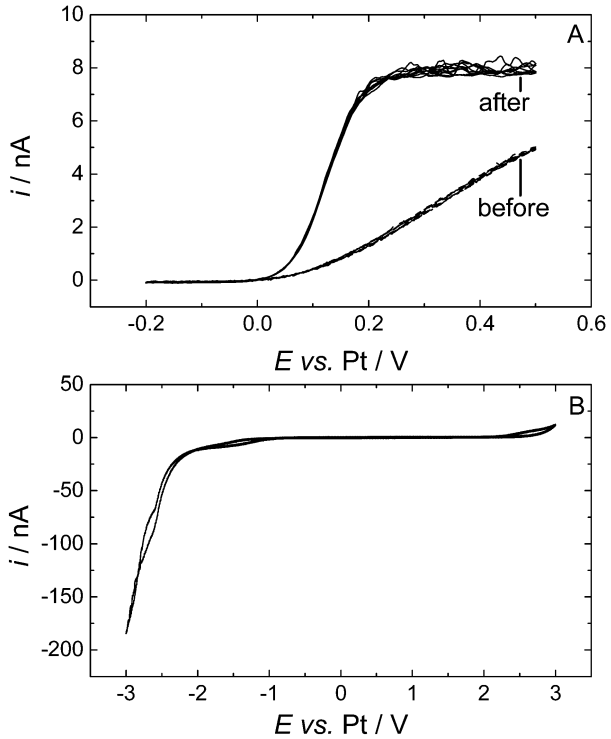

Fig. 1 Cyclic voltammetry of 0.43 mM DMFc in supercritical CO_2 with 15 wt% MeCN containing 20 mM $[NBu^n_4][BF_4]$ supporting electrolyte at 309 K. The working electrodes was a 25 μm diameter platinum disc, the counter and reference electrode were 0.5 mm diameter platinum wires. $p_A \approx 17.50$ MPa, $p_B = 17.43$ MPa. Voltammograms for (A) were recorded at 10 mV s^{-1}, (B) at 100 mV s^{-1}.

the voltammetry and that it takes some time (of the order of 1/2 day) to assemble the high pressure cell, load it with electrolyte, reagent, acetonitrile and CO_2 and then to bring it up to temperature and pressure.

3.2 Electrochemistry of decamethylferrocene in $scCO_2$ with 15 wt% CH_3CN

Cyclic voltammetry, at all three sizes of microdisc, gave stable, reproducible results. Fig. 2 shows typical cyclic voltammograms for all three sizes of Pt microdisc. For each size of electrode we observe well behaved voltammetry with a well-defined sigmoidal wave as expected for the steady state response at a microelectrode but with a limiting current plateau that is noisy and never settles to a stable value. The magnitude of the noise is larger at the larger electrode.

The noise seen on the limiting current is attributed to natural convection of the supercritical fluid mixture – a process which has a significant influence because of the low viscosity of the supercritical fluid and which is presumably driven by temperature gradients within the high pressure cell. Running repeated voltammetric scans allows us to build up an averaged current response, Fig. 3. Then to estimate the diffusion limited current we recognise that the convection causes additional transport of material to the microdisc surface and therefore only increases the current. We therefore take the lower bound

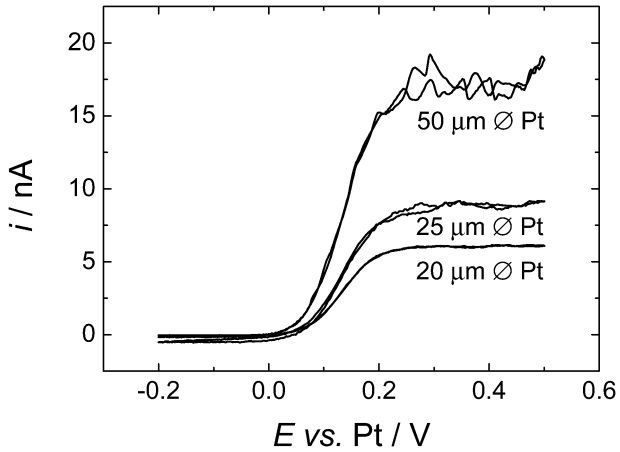

Fig. 2 Cyclic voltammetry of 0.43 mM DMFc in supercritical CO_2 with 15 wt% MeCN containing 20 mM $[NBu^n_4][BF_4]$ supporting electrolyte at 309 K. The working electrodes were a 20, 25 and 50 μm diameter platinum disc, the counter and reference electrode were 0.5 mm diameter platinum wires. $p = 17.51$ MPa, $p = 17.55$ MPa, $p = 17.60$ MPa respectively. Sweep rate 10 mV s^{-1} for all electrodes.

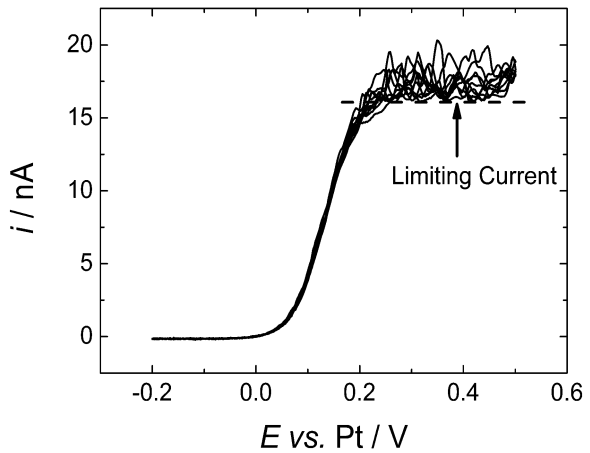

Fig. 3 Cyclic voltammograms in 0.43 mM DMFc in supercritical CO_2 with 15 wt% MeCN containing 20 mM $[NBu^n_4][BF_4]$ supporting electrolyte. $T = 309$ K. $p = 17.60$ MPa. The working electrodes was a 50 μm diameter platinum disc, the counter and reference electrode were 0.5 mm diameter platinum wires. Sweep rate 10 mV s^{-1}.

of the current in the plateau region as the best estimate of i_L, the diffusion limited current at the microdisc.

Microdisc voltammograms were analysed in the standard way by making mass transport corrected Tafel plots (plots of $\ln((i_L/i) - 1)$ against E, where i_L is the diffusion limited current and i is the measured current at potential E). This yields a straight line plot with an intersection on the potential axis of E', with a gradient of nF/RT. Voltammograms obtained for two different concentrations of DMFc (0.22 and 0.43 mM) and two different sizes of Pt microdisc electrode (25 and 50 μm diameter) were analysed and the results are given in Table 1.

From the results in Table 1 we can see that the DMFc behaves as an ideally reversible system at the lower concentration (0.22 mM) but that on increasing the higher concentration it starts to deviate from ideality and we find $n < 1$.

Table 1 Mass transport corrected Tafel analysis for DMFc at Pt microdisc electrodes in supercritical CO_2 with 15 wt% MeCN, 20 mM $[NBu^n_4][BF_4]$. T = 309 K. p = 17.24–17.72 MPa supercritical CO_2/MeCN

[DMFc]/mM	Electrode diameter/μm	n	E' *vs.* Pt/V ± 0.002 V
0.22	25	0.998 (±0.004)	0.119
	50	1.03 (±0.01)	0.110
0.43	25	0.900 (±0.002)	0.131
	50	0.910 (±0.006)	0.132

3.3 Electrochemistry of decamethylferrocene in $scCO_2$ with 15 wt% CH_3CN using a microdisc electrode with a baffle

In order to clearly demonstrate that the instability in the limiting current seen at microdisc electrodes was due to natural convection we constructed a microdisc electrode with a baffle around the end – for details of the construction see the Experimental Section. The baffle comprises an extended piece of PEEK tubing which surrounds the working electrode and extends approximately 5 mm beyond the face of the electrode and surrounding insulation. In this case a 50 μm diameter Pt disc electrode was used encased in 1/16″ diameter insulating sheath. Fig. 4 shows voltammograms recorded at the electrode fitted with the baffle and a nominally identical Pt microdisc electrode recorded in the same cell during the same supercritical experiment. Note both electrodes were preconditioned as described above to clean the electrode surface before recording the voltammograms. As the figure shows, for the microdisc fitted with the baffle a stable steady state limiting current plateau is obtained although this limiting current is slightly below the minimum plateau current on the "bare" microdisc.

The slight difference in limiting currents at the two electrodes is due to differences in their radii. This was confirmed by comparing the voltammetry for the two electrodes in aqueous ruthenium(III) hexamine solution. The two limiting currents were measured from the ruthenium hexamine trichloride system, the difference between them was found to be i_L(NB,Ru)/i_L(B,Ru) = 1.07, where NB refers to "no baffle" and B to "baffle".

3.4 Determination of the diffusion coefficient of decamethylferrocene in $scCO_2$ with 15 wt% CH_3CN

The diffusion controlled limiting current at a microdisc[35] is given by

$$i_L = 4nFDca \quad (1)$$

where i_L is the diffusion limited current, n is the number of e^- transferred, F is the Faraday constant, D is the diffusion coefficient, c is the concentration and a is the radius of the microdisc. In order to confirm that the DMFc system obeys eqn (1) we have measured the limiting currents as a function of concentration, c, and microelectrode radius, a.

Fig. 5 shows the plot obtained for the diffusion limited current against the concentration of DMFc over the range 0.22 to 11 mM for three different microdisc electrodes. As we can see the limiting current increases linearly with concentration in all cases as expected from eqn (1). The results also clearly show that the solubility of DMFc in $scCO_2$/MeCN under these conditions exceeds 11 mM. From the slopes of the plots in Fig. 5 and using eqn (1) we obtain the values for D given in Table 2.

Fig. 6 shows a plot of the limiting current as a function of microelectrode radius for a separate set of experiments using five different DMFc concentrations. Again we can see that the results are fully consistent with eqn (1). The diffusion coefficients obtained from the slopes of the lines in Fig. 6 are given in Table 3.

From the two sets of experiments (a total of eight separate experiments carried out over two weeks) we find excellent agreement in the values of D for DMFc of 4.05 × 10^{-5} cm^2 s^{-1}. This is comparable to diffusion coefficients previously reported in

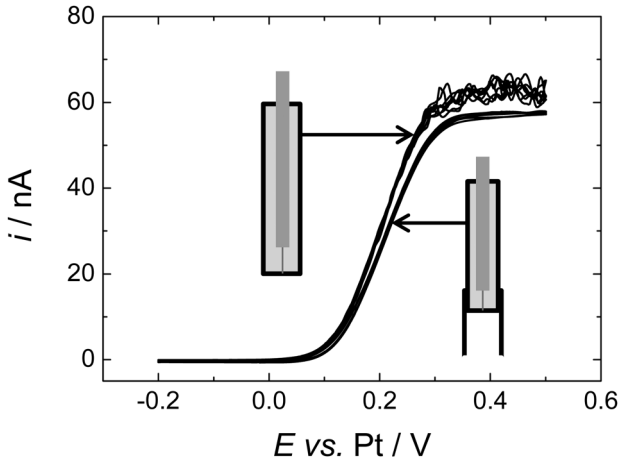

Fig. 4 Cyclic voltammetry in 1.42 mM DMFc in supercritical CO_2 with 15 wt% MeCN containing 20 mM $[NBu^n_4][BF_4]$ supporting electrolyte at 309 K. The working electrodes were both nominally 50 μm diameter platinum discs with and without a baffle, the counter and reference electrode were 0.5 mm diameter platinum wires. p = 17.58 MPa, p = 17.49 MPa respectively. Sweep rate 10 mV s^{-1} for all electrodes.

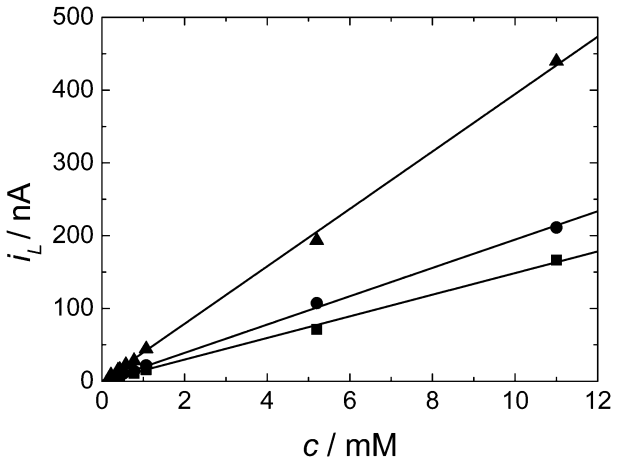

Fig. 5 Plot of diffusion limited current *versus* the decamethylferrocene concentration for a series of cyclic voltammograms in supercritical CO_2 with 15 wt% MeCN and 20 mM $[NBu^n_4][BF_4]$ electrolyte. T = 309 K. p = 17.24–17.72 MPa. The working electrodes were a 20 (■), 25 (●) and 50 μm (▲) diameter platinum disc, the counter and reference electrode were 0.5 mm diameter platinum wires.

Table 2 Variation of the diffusion coefficient with concentration of DMFc. The working electrodes were a 20, 25 and 50 μm diameter platinum disc, the counter and reference electrode were 0.5 mm diameter platinum wires. Solutions were supercritical CO_2 with 15 wt% MeCN, 20 mM $[NBu^n_4][BF_4]$. T = 309 K. p = 17.24–17.72 MPa

a/μm	D/cm^2 s^{-1}
9.5 ± 0.1	$4.05 \times 10^{-5} \pm 0.046 \times 10^{-5}$
12.64 ± 0.2	$3.99 \times 10^{-5} \pm 0.064 \times 10^{-5}$
24.72 ± 0.4	$4.14 \times 10^{-5} \pm 0.070 \times 10^{-5}$
Mean	$4.06 \times 10^{-5} \pm 0.06 \times 10^{-5}$

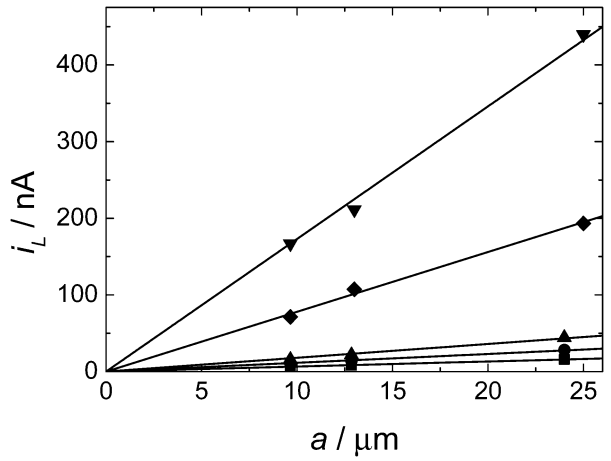

Fig. 6 Plot of diffusion limited current *versus* the electrode radii for a series of cyclic voltammograms in supercritical CO_2 with 15 wt% MeCN and 20 mM $[NBu^n_4][BF_4]$ electrolyte. T = 309 K. p = 17.24–17.72 MPa. The concentrations were 0.43 (■), 0.78 (●), 1.07 (▲), 5.20 (◆), and 11.0 mM (▼). The counter and reference electrode were 0.5 mm diameter platinum wires.

Table 3 Variation of the diffusion coefficient with electrode radii. The working electrodes were a 20, 25 and 50 μm diameter platinum disc, the counter and reference electrode were 0.5 mm diameter platinum wires. Solutions were supercritical CO_2 with 15 wt% MeCN, 20 mM $[NBu^n_4][BF_4]$. T = 309 K. p = 17.24–17.72 MPa

c/mM	D/cm^2 s^{-1}
0.43 ± 0.018	$3.96 \times 10^{-5} \pm 0.16 \times 10^{-5}$
0.78 ± 0.018	$3.81 \times 10^{-5} \pm 0.085 \times 10^{-5}$
1.07 ± 0.018	$4.37 \times 10^{-5} \pm 0.078 \times 10^{-5}$
5.20 ± 0.018	$3.89 \times 10^{-5} \pm 0.017 \times 10^{-5}$
11.0 ± 0.018	$4.08 \times 10^{-5} \pm 0.012 \times 10^{-5}$
Mean	$4.02 \times 10^{-5} \pm 0.07 \times 10^{-5}$

our work in $scCO_2$/MeCN under similar conditions for $[Cu(MeCN)_4]^+$ of 2.30×10^{-5} cm^2 s^{-1} with $[NBu^n_4][BF_4]$ supporting electrolyte and 3.30×10^{-5} cm^2 s^{-1} with $[NBu^n_4][B(3,5\text{-}(CF_3)_2C_6H_3)]$ supporting electrolyte.[17]

3.5 Comparison with the results of Toghill *et al.*

Recently Toghill *et al.*[7] suggested, based on their experimental data for the voltammetry of DMFc in $scCO_2$/MeCN, that a 60 μm thick liquid layer formed at the working electrode surface and that all of the voltammetry occurred within this layer. This conclusion was based on the results of voltammetry at macrodiscs at scan rates of 25–1000 mV s^{-1}.

From their results they obtained a diffusion coefficient for DMFc of 1.86×10^{-5} cm^2 s^{-1}. From our experiments with Pt microdisc electrodes there is no evidence for the presence of a liquid film at the electrode surface. We see microelectrode behaviour as a function of concentration and electrode radius which is fully consistent with the standard model. From work on SECM[36–38] we know that the current at a microdisc electrode increases by ~1.1 times its bulk value when the electrode is 4 multiples of the electrode radius from an interface at which the redox species concentration is held at the bulk value (the positive feedback case in SECM). Thus, if the mass transport limiting current in our experiments were due to transport across a thin (<100 μm) liquid film we would not see the correct dependence of limiting current on microdisc radius for electrodes up to 25 μm radius. In addition we see a strong influence of natural convection on the limiting current; this is inconsistent with the presence of a thick liquid film at the electrode surface.

To compare more directly to the work of Toghill *et al.* we also studied the voltammetry at a gold macrodisc electrode. In the case of gold electrodes we found no evidence for the formation of a polymeric film of the type seen for Pt electrodes and it was not necessary to cycle the electrode to cathodic potentials to clean the surface. Fig. 7 shows voltammograms recorded at 100, 200 and 500 mV s^{-1}. At these scan rates the voltammograms are not significantly distorted by the convection within the cell (see below) but the effects of *iR* drop are significant. The dashed lines in Fig. 7 connect the peak currents at the different scan rates and provide a simple way to correct for the effects of *iR* drop since for the reversible case the peak potentials should be independent of scan rate. The slopes of the dashed lines give an estimate of the uncompensated resistance of 0.14 MΩ which is reasonable given the known conductivity of this electrolyte.[30] The separation between the two lines is 83 mV, close to the expected value of 61.2 mV for a reversible 1e$^-$ process at 309 K. From the cyclic voltammetry at the gold macroelectrode we

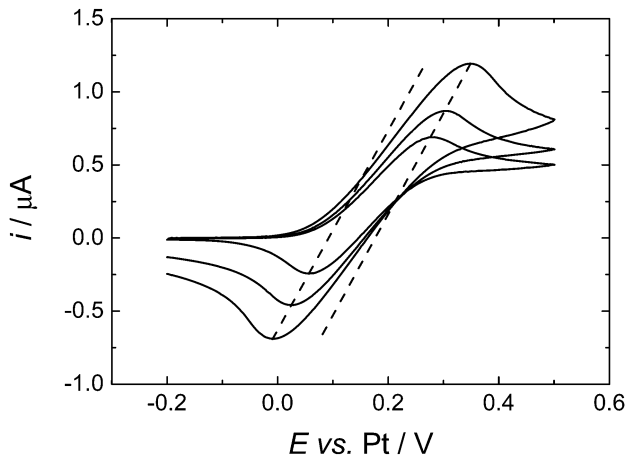

Fig. 7 Cyclic voltammograms in 0.638 mM DMFc in supercritical CO_2 with 15 wt% MeCN containing 20 mM $[NBu^n_4][BF_4]$ supporting electrolyte. T = 309 K. p = 17.51 MPa. The working electrodes was a 0.5 mm diameter gold disc, the counter and reference electrode were 0.5 mm diameter platinum wires. Sweep rate 100, 200 and 500 mV s^{-1}.

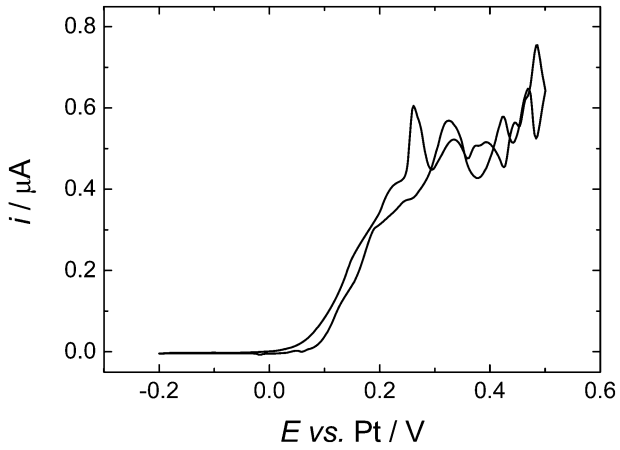

Fig. 8 Cyclic voltammetry in 0.638 mM DMFc in supercritical CO_2 with 15 wt% MeCN containing 20 mM $[NBu^n_4][BF_4]$ supporting electrolyte. T = 309 K. p = 17.51 MPa. The working electrodes was a 0.5 mm diameter gold disc, the counter and reference electrode were 0.5 mm diameter platinum wires. Sweep rate 10 mV s^{-1}.

estimate the diffusion coefficient for the DMFc to be 5.05 × 10^{-5} cm^2 s^{-1} which compares well with the results presented above for the microelectrodes. At lower scan rates the voltammetry at the gold macrodisc electrode is significantly distorted, as expected, by convection within the cell. Fig. 8 shows a voltammogram recorded at 10 mV s^{-1}. It has the sigmoidal shape expected for hydrodynamic voltammetry and shows significant noise at anodic potential where the current becomes mass transport limited.

It is important to note that there are significant differences in the experimental conditions used in our studies and those of Toghill *et al.* Toghill *et al.* used an ionic liquid electrolyte (10 mM $[N(C_{10}H_{11})_4][B(C_6F_5)_4]$) and significantly higher concentrations of acetonitrile co-solvent (up to 30 vol% in their work as compared to ~15 wt% here). Their experiments were carried out at slightly higher temperature (313 rather than 309 K) but at lower pressure (10 rather than 17 MPa). As the acetonitrile mole fraction is increased, the dielectric constant of the system increases. Thus it is crucial to add 10–18% (mole fraction) of acetonitrile into $scCO_2$ to achieve a dielectric constant of 7 to ensure sufficient dissociation of the electrolyte.[16] Adding much higher concentrations of acetonitrile ($x_{CH_3CN} > 0.5$) will significantly reduce the electrostatic solvation energy, but will also make the solution more liquid-like and therefore slow down mass transport.

Although a mole fraction of 0.41 will yield a higher dielectric constant, it also moves towards a more liquid-like system. A marked difference in the voltammetry between the results of Toghill *et al.* and the present work is the significant sloping background seen in their voltammograms (compare Fig. 2 and 3 in their paper with Fig. 2 above). The reason for this is unclear but it clearly affects their limiting current and peak current values.

4. Conclusions

We have carried out detailed studies of the voltammetry of decamethylferrocene in $scCO_2$/MeCN (15 wt%), 20 mM $[NBu^n_4][BF_4]$ at 309 K and 17.5 MPa at Pt microdisc electrodes and a gold macroelectrode. For the Pt electrodes we find that it is necessary to perform a preconditioning step to remove a passivating film initially present at the surface, but this is not necessary for the gold electrode. In all cases there is significant noise in the current at high overpotential caused by natural convection within the cell due to the low viscosity of the supercritical fluid. We are able to significantly reduce this by placing a baffle around the microelectrode electrode. For the platinum microelectrode studies we find reversible $1e^-$ redox behaviour with a formal potential of 0.115 V *vs.* Pt pseudo reference electrode. The limiting currents, corrected for the effects of convection, measured at the Pt microdisc electrodes at concentrations from 0.22 to 11 mM and for radii from 10 to 25 μm all obey the microdisc equation. From the analysis of the results we obtain a value of the diffusion coefficient of DMFc of D = 4.06 × 10^{-5} cm^2 s^{-1} in $scCO_2$/MeCN (15 wt%), 20 mM $[NBu^n_4][BF_4]$ and 309 K at 17.5 MPa. The solubility limit for DMFc under these conditions is shown to exceed 11 mM. The results obtained at the gold macroelectrode are wholly consistent with the results for the Pt microelectrodes. We therefore conclude that in $scCO_2$/MeCN (15 wt%), 20 mM $[NBu^n_4][BF_4]$ and 309 K at 17.5 MPa the electrochemistry of DMFc is well behaved and there is no evidence for the presence of a liquid film coating the electrode surface.

Acknowledgements

This work is part of the Supercritical Fluid Electrodeposition project (www.scfed.net) which is a multidisciplinary collaboration of British universities investigating the fundamental and applied aspects of supercritical fluids funding by a Programme Grant from the EPSRC (EP/I013394/1). The author would like to thank Dr Wenjian Zhang for his help with sublimation of materials. The author would also like to thank Dr Charlie Cummings for his advice on the preconditioning step. We would also like to acknowledge our team members at University of Southampton and collaborating teams at University of Nottingham and University of Warwick. PNB gratefully acknowledges the receipt of a Wolfson Merit award.

Notes and references

1 K. E. Toghill, M. A. Méndez and P. Voyame, *Electrochem. Commun.*, 2014, **44**, 27–30.
2 R. M. Crooks and A. J. Bard, *J. Electroanal. Chem.*, 1988, **243**, 117–131.
3 C. R. Cabrera and A. J. Bard, *J. Electroanal. Chem.*, 1989, **273**, 147–160.
4 A. P. Abbott and J. C. Harper, *J. Chem. Soc., Faraday Trans.*, 1996, **92**, 3895–3898.
5 A. P. Abbott, C. A. Eardley, J. C. Harper and E. G. Hope, *J. Electroanal. Chem.*, 1998, **457**, 1–4.
6 A. P. Abbott, E. G. Hope and D. J. Palmer, *Anal. Chem.*, 2005, **77**, 6702–6708.

7 K. E. Toghill, P. Voyame, D. Momotenko, A. J. Olaya and H. H. Girault, *Phys. Chem. Chem. Phys.*, 2013, **15**, 972–978.
8 D. Niehaus, M. Philips, A. Michael and R. M. Wightman, *J. Phys. Chem.*, 1989, **93**, 6232–6236.
9 S. A. Olsen and D. E. Tallman, *Anal. Chem.*, 1994, **66**, 503–509.
10 D. L. Goldfarb and H. R. Corti, *J. Phys. Chem. B*, 2004, **108**, 3368–3375.
11 M. Gattrell, N. Gupta and A. Co, *J. Electroanal. Chem.*, 2006, **594**, 1–19.
12 A. P. Abbott and C. A. Eardley, *J. Phys. Chem. B*, 2000, **104**, 775–779.
13 M. Atobe, H. Ohsuka and T. Fuchigami, *Chem. Lett.*, 2004, **33**, 618–619.
14 H. Yan, T. Sato, D. Komago, A. Yamaguchi, K. Oyaizu, M. Yuasa and K. Otake, *Langmuir*, 2005, **21**, 12303–12308.
15 P. E. Anderson, R. N. Badlani, J. Mayer and P. A. Mabrouk, *J. Am. Chem. Soc.*, 2002, **124**, 10284–10285.
16 P. N. Bartlett, D. A. Cook, M. W. George, A. L. Hector, J. Ke, W. Levason, G. Reid, D. C. Smith and W. Zhang, *Phys. Chem. Chem. Phys.*, 2014, **16**, 9202–9219.
17 D. Cook, P. N. Bartlett, W. J. Zhang, W. Levason, G. Reid, J. Ke, W. T. Su, M. W. George, J. Wilson, D. Smith, K. Mallik, E. Barrett and P. Sazio, *Phys. Chem. Chem. Phys.*, 2010, **12**, 11744–11752.
18 P. N. Bartlett, M. Perdjon-Abel, D. Cook, G. Reid, W. Levason, F. Cheng, W. Zhang, M. W. George, J. Ke, R. Beanland and J. Sloan, *ChemElectroChem*, 2014, **1**, 187–194.
19 J. Ke, P. N. Bartlett, D. Cook, T. L. Easun, M. W. George, W. Levason, G. Reid, D. Smith, W. T. Su and W. J. Zhang, *Phys. Chem. Chem. Phys.*, 2012, **14**, 1517–1528.
20 J. Ke, W. T. Su, S. M. Howdle, M. W. George, D. Cook, M. Perdjon-Abel, P. N. Bartlett, W. J. Zhang, F. Cheng, W. Levason, G. Reid, J. Hyde, J. Wilson, D. C. Smith, K. Mallik and P. Sazio, *Proc. Natl. Acad. Sci. U. S. A.*, 2009, **106**, 14768–14772.
21 C. F. Karanikas and J. J. Watkins, *Microelectron. Eng.*, 2009, **87**, 566–572.
22 A. Cabanas, D. P. Long and J. J. Watkins, *Chem. Mater.*, 2004, **16**, 2028–2033.
23 A. P. Abbott and J. C. Harper, *Phys. Chem. Chem. Phys.*, 1999, **1**, 839–841.
24 M. S. Kim, J. Y. Kim, C. K. Kim and N. K. Kim, *Chemosphere*, 2005, **58**, 459–465.
25 C. Y. Kong, M. Nakamura, K. Sone, T. Funazukuri and S. Kagei, *J. Chem. Eng. Data*, 2010, **55**, 3095–3100.
26 D. L. Goldfarb, D. P. Fernandez and H. R. Corti, *Fluid Phase Equilib.*, 1999, **158**, 1011–1019.
27 H. Ohde, F. Hunt, S. Kihara and C. M. Wai, *Anal. Chem.*, 2000, **72**, 4738–4741.
28 J. M. Blackburn, D. P. Long, A. Cabanas and J. J. Watkins, *Science*, 2001, **294**, 141–145.
29 H. Wakayama and Y. Fukushima, *Ind. Eng. Chem. Res.*, 2006, **45**, 3328–3331.
30 P. N. Bartlett, D. C. Cook, M. W. George, J. Ke, W. Levason, G. Reid, W. T. Su and W. J. Zhang, *Phys. Chem. Chem. Phys.*, 2009, **12**, 492–501.
31 A. O'Neil and J. J. Watkins, *Chem. Mater.*, 2007, **19**, 5460–5466.
32 E. T. Hunde and J. J. Watkins, *Chem. Mater.*, 2004, **16**, 498–503.
33 A. C. Michael and R. M. Wightman, *Anal. Chem.*, 1989, **61**, 2193–2200.
34 I. Noviandri, K. N. Brown, D. S. Fleming, P. T. Gulyas, P. A. Lay, A. F. Masters and L. Phillips, *J. Phys. Chem. B*, 1999, **103**, 6713–6722.
35 G. Denuault, M. V. Mirkin and A. J. Bard, *J. Electroanal. Chem.*, 1991, **308**, 27–38.
36 C. Lefrou and R. Cornut, *ChemPhysChem*, 2010, **11**, 547–556.
37 J. L. Amphlett and G. Denuault, *J. Phys. Chem. B*, 1998, **102**, 9946–9951.
38 A. J. Bard and M. V. Mirkin, *Scanning Electrochemical Microscopy*, Marcel Dekker, Inc., New York, 2001.